Preprint
UCRL-JC-135773

Gamma-Ray Spectrometers using a Bulk Sn Absorber Coupled to a Mo/Cu Multilayer Superconducting Transition Edge Sensor

D.T. Chow, M.A. Lindeman, M.F. Cunningham, M. Frank, T.W. Barbee, S.E. Labov

U.S. Department of Energy
Lawrence Livermore National Laboratory

This article was submitted to Eighth International Workshop on Low Temperature Detectors LTD-8, Dalfsen, The Netherlands, August 15-20, 1999

September 21, 1999

This work was performed under the auspices of the United States Department of Energy by the University of California, Lawrence Livermore National Laboratory under contract No. W-7405-Eng-48.

Gamma-ray Spectrometers Using a Bulk Sn Absorber Coupled to a Mo/Cu Multilayer Superconducting Transition Edge Sensor

D.T. Chow[1,2], M.A. Lindeman[1,2], M.F. Cunningham[1,2], M. Frank[1], T.W. Barbee, Jr[1]., S.E. Labov[1]

[1]Lawrence Livermore National Laboratory
Livermore, CA 94550
USA

[2]Department of Applied Science
University of California, Davis
Livermore, CA 94550
USA

Abstract

We are developing gamma-ray detectors with a bulk absorber and a superconducting transition-edge sensor. The absorber is high purity Sn and the transition-edge sensor is a Mo/Cu multilayer thin film. We have characterized the detector, and will discuss x-ray and gamma-ray results.

1. Introduction

At the Lawrence Livermore National Laboratory, we are interested in the development of gamma-ray spectrometers for nuclear nonproliferation and arms control programs. Nuclear materials intended for different purposes have different isotopic abundances. High energy resolution gamma-ray spectrometers can be used to determine the composition of nuclear materials to high accuracy. The resolution of commercial germanium ionization detectors, which is limited to 300 eV full width at half maximum (FWHM) for 60 keV photons, is often insufficient for this application. Furthermore, their linewidths increase with energy.

We are developing low temperature microcalorimeters for high resolution gamma-ray spectrometry. Their energy resolution is limited by the thermal fluctuations to $\Delta E \sim 2.35\sqrt{kT^2C}$, where k is Boltzmann's constant, T is the operating temperature, and C is the heat capacity of the device. At low temperatures, superconductors have very small heat capacities, making them ideal materials for microcalorimeters. In our detector design, the theoretical linewidth is on the order of 20 eV, operating at 0.1 K. Furthermore, the linewidth is independent of incident photon energy, allowing high resolution over a large energy range.

2. Detector design

A microcalorimeter consists of an absorber, a sensitive thermometer, and a weak thermal link to a cold bath. We use a 300 x 300 x 250 μm^3 high-purity bulk Sn absorber[1]. The absorption efficiency is over 70% for 60 keV gamma-rays. Our thermometer is a superconducting transition edge sensor (TES) operated on the narrow transition between normal and superconducting state, where small changes in temperature cause a large change in resistance. The TES is a multilayer superlattice of alternating Mo and Cu[2]. These two materials are immiscible, allowing the fabrication of a stable thin film which can be annealed. The transition temperature (T_C) is governed by the proximity effect and can be tuned by varying the Mo/Cu ratio. In our TES, there are 23 Cu layers, each 70Å thick, and 20 Mo layers, each 20Å thick. A film with this Mo/Cu ratio has T_C = 100 mK. The bulk Sn absorber is attached to the TES with Stycast 2850FT epoxy. The Stycast is approximately 300μm in diameter and 10 μm thick. After curing, Stycast exerts stress on the Mo/Cu film, lowering T_C to ~80 mK. The absorber and TES are weakly coupled to a cold bath via a 0.5 μm thick silicon (SiN) membrane. In our detector design, the thermal conductivity of the SiN membrane is G_{SiN} = 0.5 nW/K. Electrical contact to the TES is made by thin film superconducting Al leads with very low thermal conductivity G_{Al}, so that thermal conductivity of the weak link $G_{link} = G_{SiN} + G_{Al}$ is dominated by the SiN membrane.

3. Experimental setup

The detector was tested in an adiabatic demagnetization refrigerator (ADR) with a base temperature below 60 mK. The TES is voltage biased, allowing negative electrothermal feedback to stabilize the TES on the transition[3]. Incident gamma rays cause a change in the resistance of the TES and subsequently the current through the TES. This current is measured with a Hypres model #30 single-stage 208 series array SQUID with noise less than 10 $pA/Hz^{1/2}$.

4. Detector characteristics

Figure 1 shows the current-voltage characteristics of the detector at different bath temperatures. At high bias, the device assumes its normal resistance of R_n = 0.33 Ω. At low bias, the device becomes superconducting and exhibits a supercurrent. Since the SQUID read-out circuit is a 2-wire measurement, the IV curves exhibit a lead resistance of 12 mΩ. Each IV curve is taken at a

constant bath temperature. Due to the voltage bias, the device operates near constant power in the superconducting transition between supercurrent and R_n. Radial lines emanating from the origin are lines of constant resistance. The family of IV curves has effectively two independent parameters: operating resistance (R_{op}) and power (P_{op}). We examine device characteristics as a function of these two parameters.

From the operating current I_{op}, voltage V_{op}, and bath temperature T_{bath}, we calculate resistance R_{op}, power P_{op}, and the thermal conductivity of the weak link G_{Link}. The measured gamma-ray pulses of a given energy E allow inferring the change in current dI and change in resistance dR. The heat capacity C is given by device geometry. From these parameters, we can construct the resistance as a function of temperature and current, $R_{TES}(T,I)$.

An important parameter for microcalorimeters is $\alpha = (T_{op}/R_{op})(dR/dT)$. This parameter is dependent on current, as larger currents tend to broaden the superconducting transition. Experimentally, we calculate $T_{op} = T_{bath} + P_{op}/G_{link}$ from the measured thermal conductivity of the weak link, R_{op} is taken from the IV curves, dT = E/C is known from the incident gamma-ray energy, and dR is inferred from the pulse height.

We first examine current pulse data taken at different bias points on one specific IV curve measured at constant T_{bath}. This effectively holds P_{op} constant while changing R_{op}. The current pulse due to a change in temperature is given by

$$dI = -(P\alpha/VT)dT.$$

In this case, P, T, and V are effectively constant. As R_{op} changes from zero to R_n, large changes in α result. Figure 2 shows a plot of pulse height vs. α. There is a linear correlation between the parameter α and the pulse height, as expected.

Similarly, by holding R_{op} constant and changing the bath temperature, we can measure pulse height as P_{op} changes (figure 3). The correlation is not linear because at higher P_{op}, the current is increased. As I_{op} increases, the transition width broadens and reduces the value of α. This analysis allows us to choose a bias point for maximum pulse height and signal-to-noise ratio.

5. Device modeling

The detector may be modeled by a set of differential equations based on a thermal circuit in which the temperature T of the various detector components is determined by their respective heat capacities C and the thermal conductivity G between them (figure 4)[4].

$$\frac{d}{dt}T_0 = \frac{G_{Kapitza}}{C_{Absorber}}(T_0 - T_1)$$

$$\frac{d}{dt}T_1 = \frac{G_{Kapitza}}{C_{Stycast}}(T_1 - T_2) + \frac{G_{Kapitza}}{C_{Stycast}}(T_0 - T_1)$$

$$\frac{d}{dt}T_2 = \frac{G_{e-ph}}{C_{phTES}}(T_2 - T_3) + \frac{G_{SiN} + G_{Al}}{C_{phTES}}(T_2 - T_{Bath}) + \frac{G_{Kapitza}}{C_{phTES}}(T_1 - T_2)$$

$$\frac{d}{dt}T_3 = \frac{G_{ep}}{C_{e^-TES}}(T_3 - T_2) + \frac{V_{op}^2}{C_{phTES}R_{TES}(T_3)}$$

The electrons (e^- TES) and the phonons (ph TES) of the TES have different temperatures but are linked by electron-phonon coupling $G_{e\text{-}ph}$. Only the electron temperature determines the electrical characteristics of the TES.

All parameters are calculated from published material properties except for the thermal conductance of the SiN membrane G_{SiN} and the resistance of the TES $R_{TES}(T_3)$, which are measured experimentally. This set of differential equations is solved numerically to give the temperature profile in the TES upon the absorption of a gamma ray.

The heat capacity of the detector is dominated by the Stycast epoxy, with $C_{Stycast}$ = 145 keV/mK. The limiting thermal conductivity is G_{SiN} = 0.5 nW/K. Neglecting all other parameters, we can find an approximate analytical solution of the temperature profile[3]. The peak current is then given by

$$dI \approx \frac{V_{op}\alpha E}{C R_{op} T_{op}} \approx 5\mu A ,$$

and the decay time with electrothermal feedback is

$$\tau \approx \frac{C T}{\alpha G P}\frac{dP}{dT} \approx 3ms .$$

The inset in figure 4 shows that the modeled pulse (dotted line) agrees reasonably well with a measured pulse (solid line). The largest uncertainty in the calculations lies in estimating the heat capacity of the Stycast. If the heat capacity were smaller, the pulse height would be larger, but the decay time would be shorter, and vice versa.

6. Gamma-ray spectrum

A spectrum from an ^{241}Am source is shown in figure 5. We observe 60 keV gamma rays from ^{241}Am as well as L-lines from the decay product Np. Since the absorber is made of Sn, there are Sn escape lines in the spectrum. The energetic Np L-lines also excite Cu fluorescence from the detector mount.

The measured spectrum exhibits non-linearity at high energy (figure 6). This is due to the fact that high energy pulses produce a change in temperature large enough that it extends beyond the steep part of the superconducting transition of the TES.

With optimal bias and filtering, the best energy resolution achieved is 230 eV for 59.54 keV gamma rays (figure 6 inset). The signal-to-noise ratio of these gamma-ray pulses exceeds 500. However, the non-linearity of the TES decreases the gain of the detector at high energy, resulting in a degraded resolution. Fluctuations of the bias point also contribute noise to the measurements, since maintaining a steady voltage bias for a low operating resistance (R_{op} = 50 mΩ) is challenging. Position dependence in the absorber will also broaden the linewidth.

The measured electronic baseline noise of the detector is 150 eV. Calculated Johnson noise and SQUID noise have very small contributions of 2.5 eV and 2 eV, respectively. Phonon noise for this detector contributes 20 eV. The discrepancy between the quadrature sum of the calculated noise sources and the measured baseline noise is attributed to 60 Hz pick-up, 1/f noise, and possibly phase slips in the TES.

7. Conclusion

We have developed a prototype superconducting gamma-ray microcalorimeter with a high-purity bulk Sn absorber coupled to a Mo/Cu multilayer TES. The measured resolution is 230 eV for 60 keV gamma rays. We showed measurements of signal size as functions of bias parameters such as α and power. We have measured the parameter α as a function of operating power. We find that α decreases with increasing operating power due the broadening of the transition with high operating current. A realistic microcalorimeter model must therefore include the current dependence of α.[5]

8. Acknowledgments

Many thanks to Jan Batteux for excellent experimental and technical support. This work was performed under the auspices of the U.S. Department of Energy by Lawrence Livermore National Laboratory under contract No. W-7405-ENG-48.

References

[1] Egelhof, P., Beyer, H.F., McCammon, D., Feilitzsch, F. v., et al. (1996) Application of low temperature calorimeters for precise Lamb shift measurements on hydrogen-like very heavy ions. *Nucl. Instr. Meth.* **A370**, 263-265.

[2] Cunningham, M.F., et al. (1999) Proceedings of the 8th International Workshop on Low Temperature Detectors.

[3] Irwin, K.D., Hilton, G.C., Wollman, D.A., Martinis, J.M. (1996) X-ray detection using a superconducting transition-edge sensor microcalorimeter with electrothermal feedback. *Appl. Phys. Lett.* **69**, 1945-1947.

[4] Pröbst, F., Frank, M., Cooper, S., Colling, P., Dummer, D., Ferger, P., Forster, G., Nuciotti, A., Seidel, W., Stodolsky, L. (1995) Model for cryogenic particle detectors with superconducting phase transition thermometers. *J. Low Temp. Phys.*, **100**,69

[5] Lindeman, M.A., Labov, S.E., Frank, M. (1999) A comprehensive model for low-temperature calorimeters. Submitted to *J. Appl. Phys.*

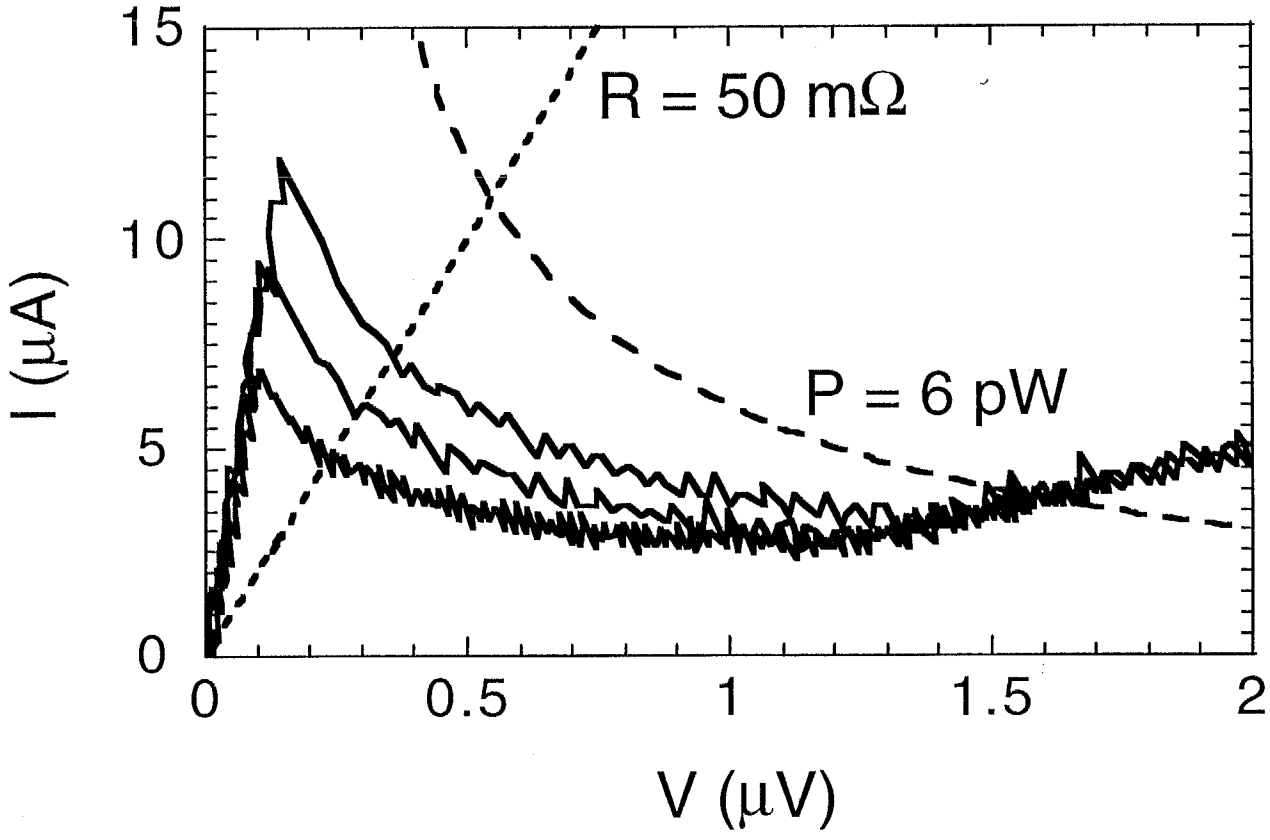

Figure 1

Several IV curves (solid) traced at different bath temperatures. Also shown is a line of constant resistance (dotted) and constant power (dashed).

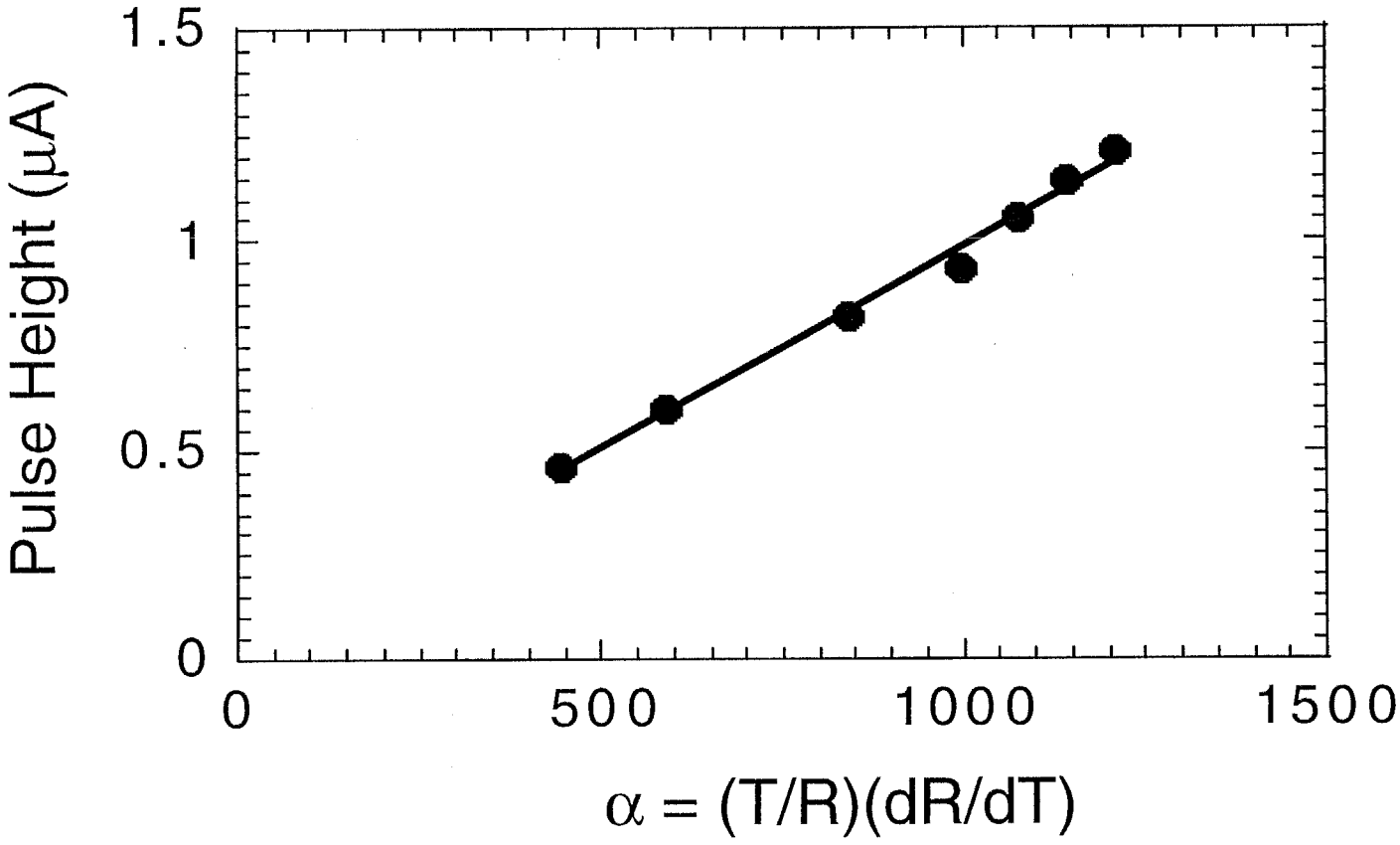

Figure 2

Pulse height as a function of α. Pulse data are taken by changing the operating resistance of the TES while keeping bath temperature constant.

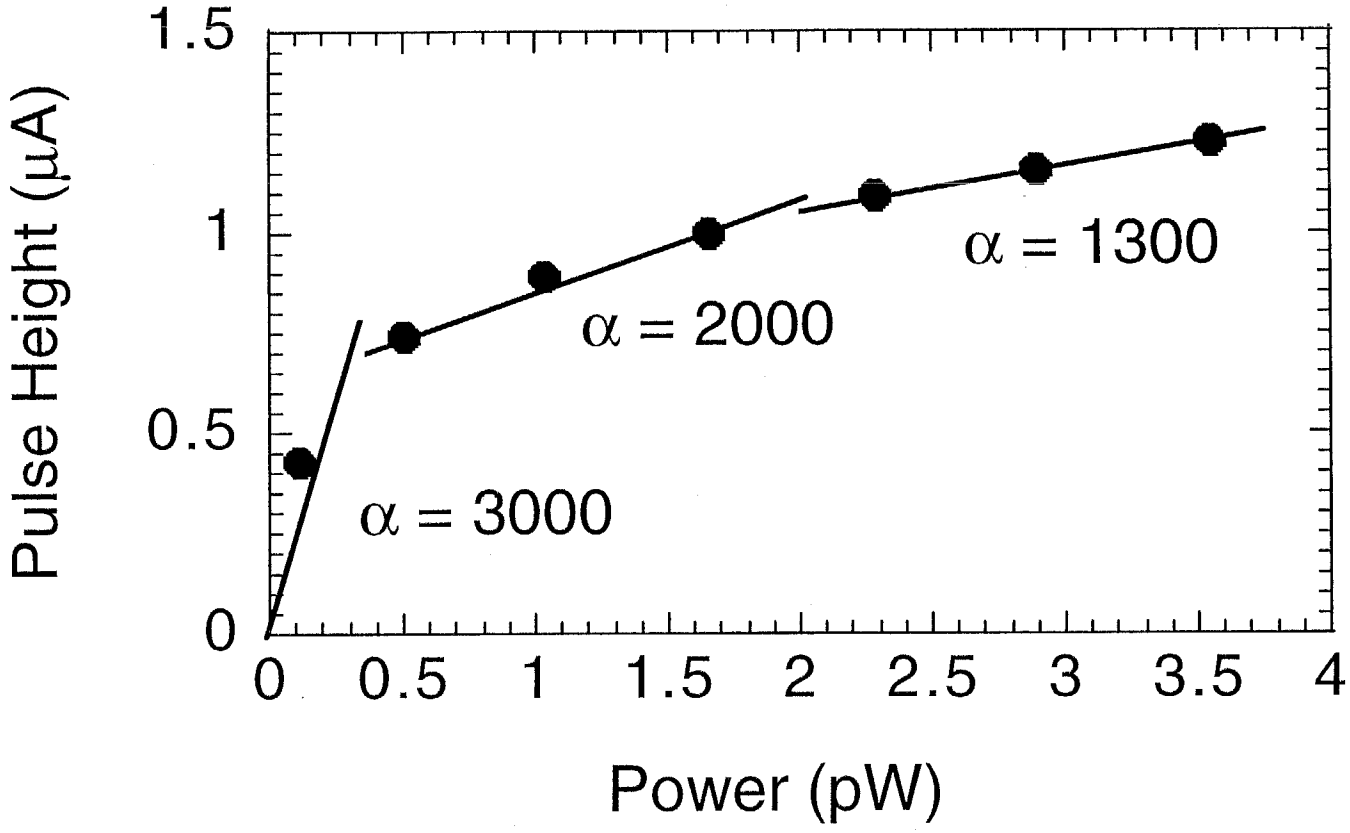

Figure 3

Pulse height as a function of operating power. Pulse data are taken by changing the bath temperature while keeping operating resistance of the TES constant.

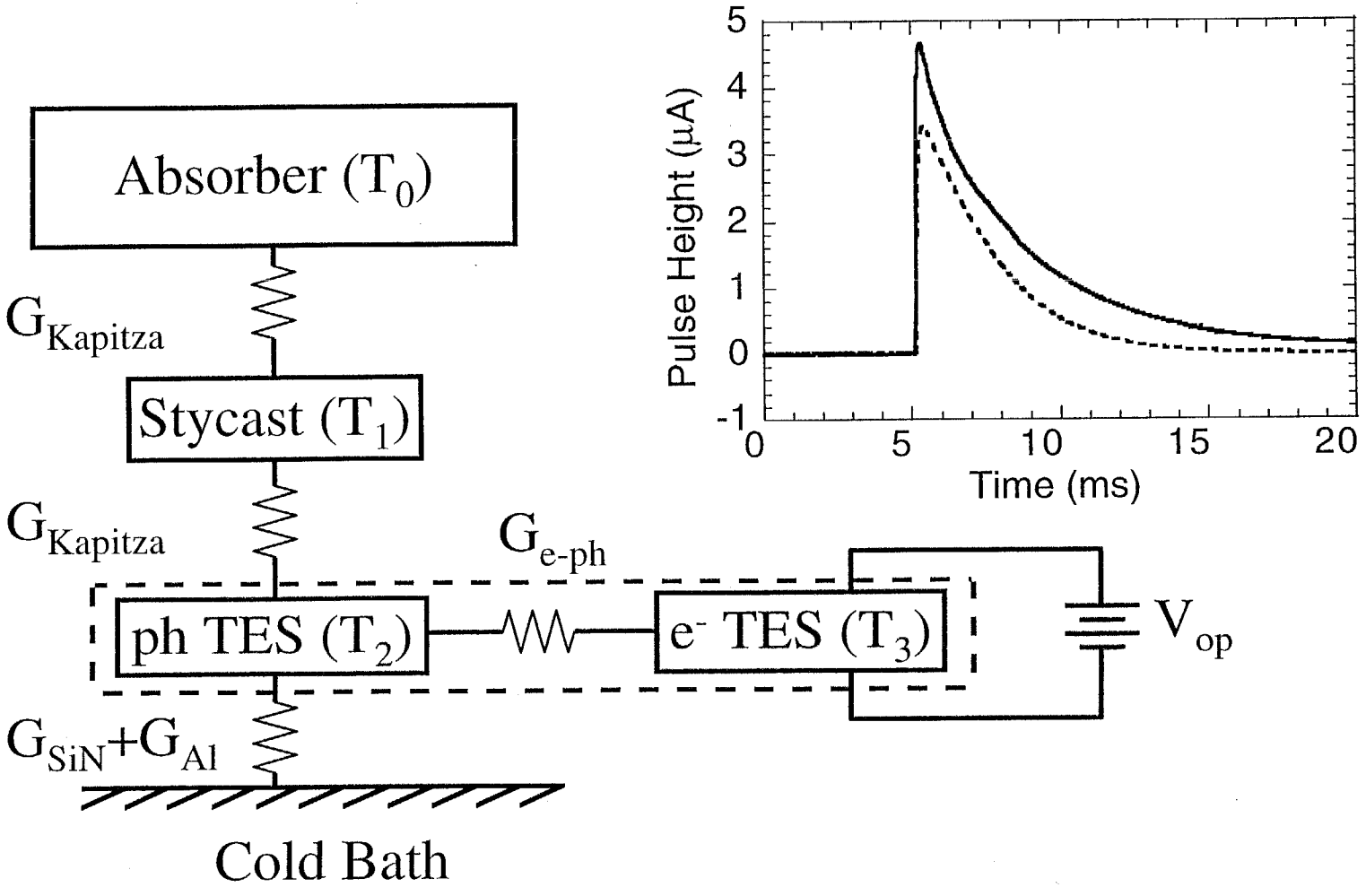

Figure 4

Thermal circuit of the detector showing various components of the detector and the thermal coupling between them. Inset shows modeled pulse (dashed line) compared with measured pulse (solid line).

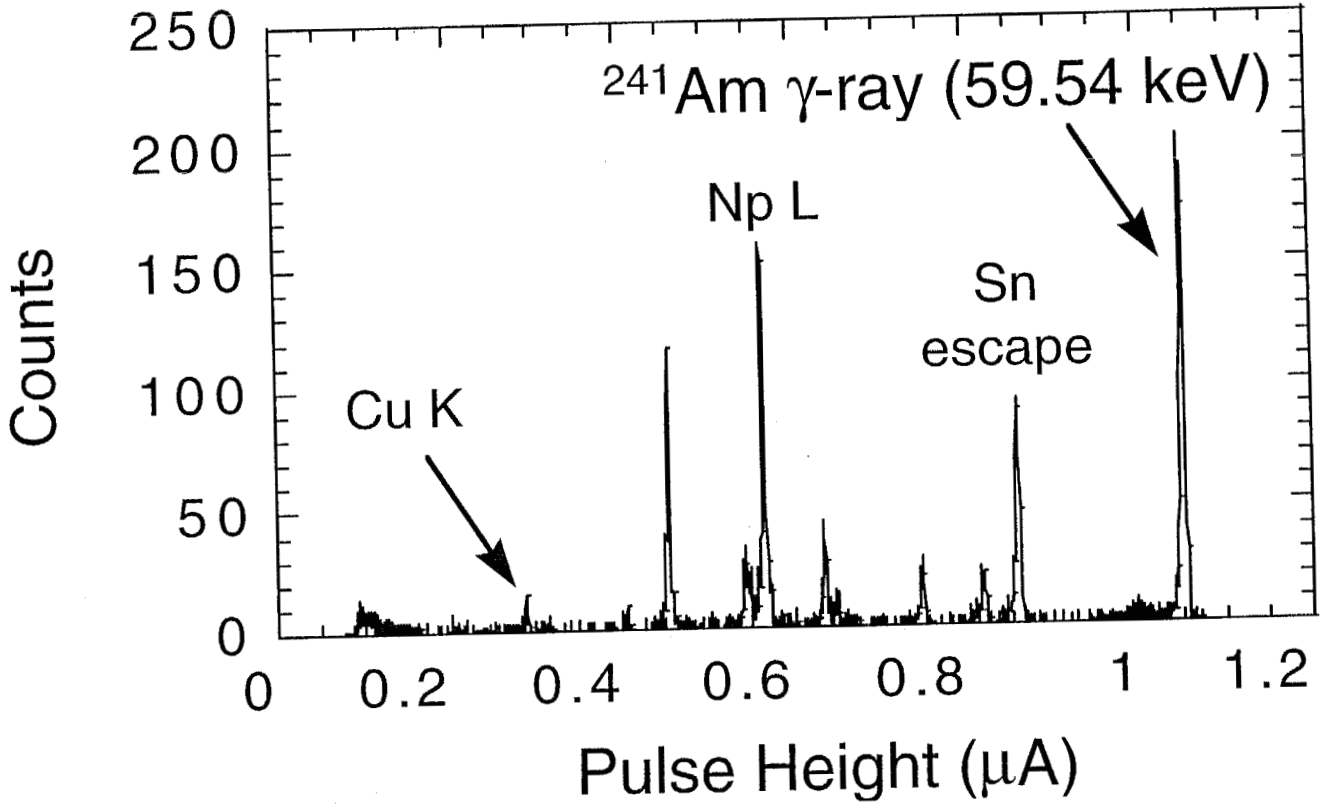

Figure 5

Spectrum of ^{241}Am showing 60 keV Am gamma-rays, Sn escape lines, Np L-lines, and a Cu fluorescence K-line.

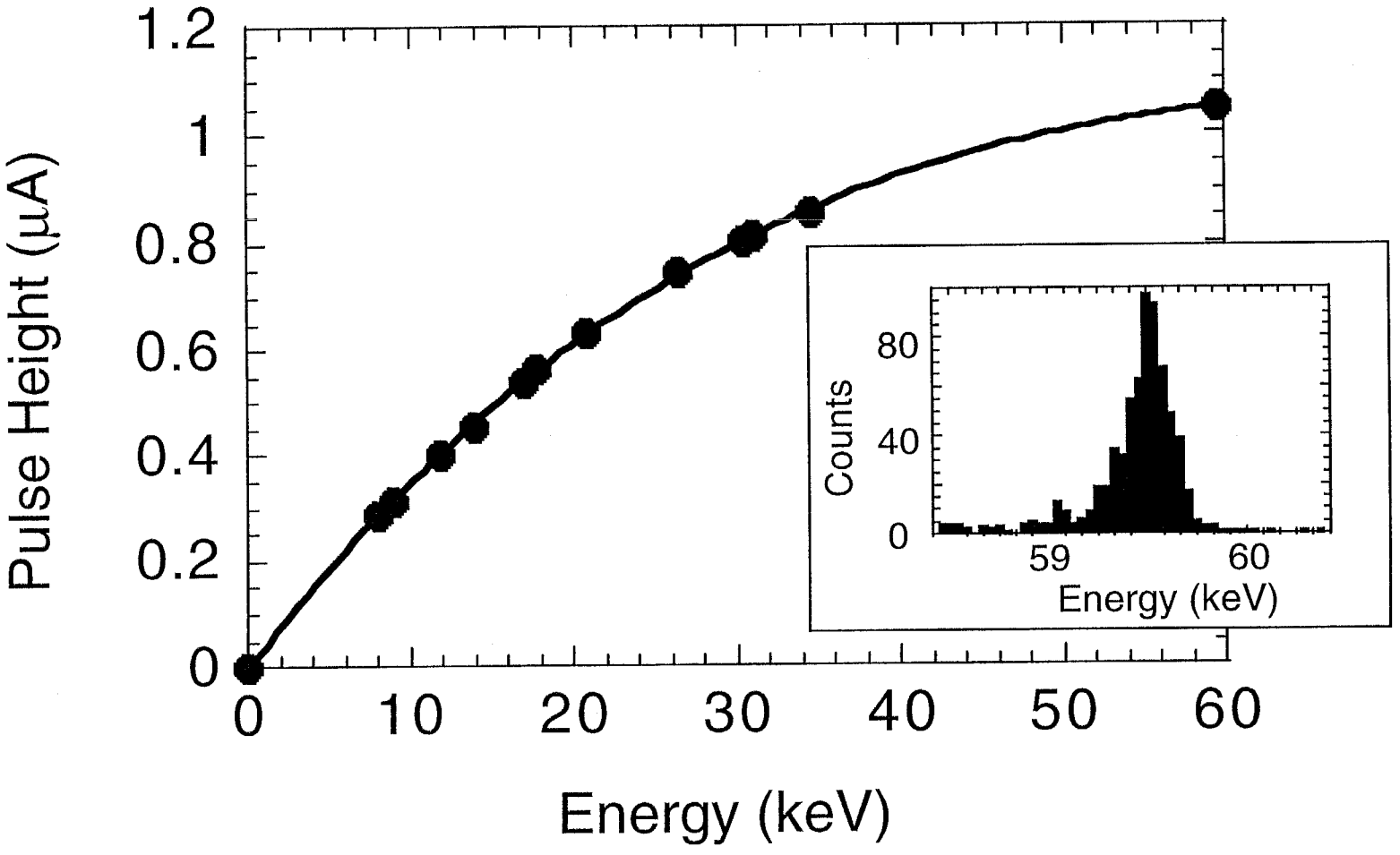

Figure 6

Non-linear response of the detector as a function of incident photon energy. Inset shows 60 keV line under optimal operating conditions.